HHS Public Access

Author manuscript

Curr Biol. Author manuscript; available in PMC 2023 November 21.

Published in final edited form as:

Curr Biol. 2022 November 21; 32(22): 4783–4796.e3. doi:10.1016/j.cub.2022.09.016.

Post-developmental plasticity of the primary rod pathway allows restoration of visually guided behaviors

Yan Cao[1], **Diego Fajardo**[2], **Debbie Guerrero-Given**[3], **Melanie A. Samuel**[4], **Toshihisa Ohtsuka**[5], **Shannon E. Boye**[2], **Naomi Kamasawa**[3], **Kirill A. Martemyanov**[1,*]

[1]Department of Neuroscience, UF Scripps Biomedical Research, Jupiter, FL 33458 USA

[2]Division of Cellular and Molecular Therapy, Department of Pediatrics, University of Florida, Gainesville, FL, USA

[3]The Imaging Center, Electron Microscopy Core Facility, Max Planck Florida Institute, 1 Max Planck Way, Jupiter, FL 33458 USA.

[4]Department of Neuroscience, Huffington Center on Aging, Baylor College of Medicine, One Baylor Plaza, Houston, Texas 77030, USA

[5]Department of Biochemistry, Graduate School of Medicine/Faculty of Medicine, University of Yamanashi, 409-3898 Japan

Summary

Formation of neural circuits occurs in a programmed fashion, but proper activity in the circuit is essential for refining the organization necessary for driving complex behavioral tasks. In the retina, sensory deprivation during the critical period of development is well known to perturb organization of the visual circuit making the animals unable to use vision for behavior. However, the extent of plasticity, molecular factors involved and malleability of individual channels in the circuit to manipulations outside of the critical period are not well understood. In this study we selectively disconnected and reconnected rod photoreceptors in mature animals after completion of the retina circuit development. We found that introducing synaptic rod photoreceptor input post-developmentally allowed their integration into the circuit both anatomically and functionally. Remarkably, adult mice with newly integrated rod photoreceptors gained high sensitivity vision even when it was absent from birth. These observations reveal plasticity of the retina circuit organization after closure of the critical period and encourage development of vision restoration strategies for congenital blinding disorders.

[*]Correspondence and Lead Contact: Dr. Kirill Martemyanov: kmartemyanov@ufl.edu.

Author Contributions

Y.C. designed and performed all immunohistochemical, electrophysiological and biochemical experiments and analyzed the data, D.F. performed viral injections, D.G-G. and N.K. performed electron microscopy experiments and analysis, M.A.S. and T.O. contributed key reagents – genetically engineered mice and their tissues, S.E.B. generated viruses and supervised D.F., K.A.M. conceived this study, analyzed the results and wrote the manuscript with the help of all authors. All authors contributed to editing the manuscript.

Declaration of interests

The authors declare no competing interests.

Graphical Abstract

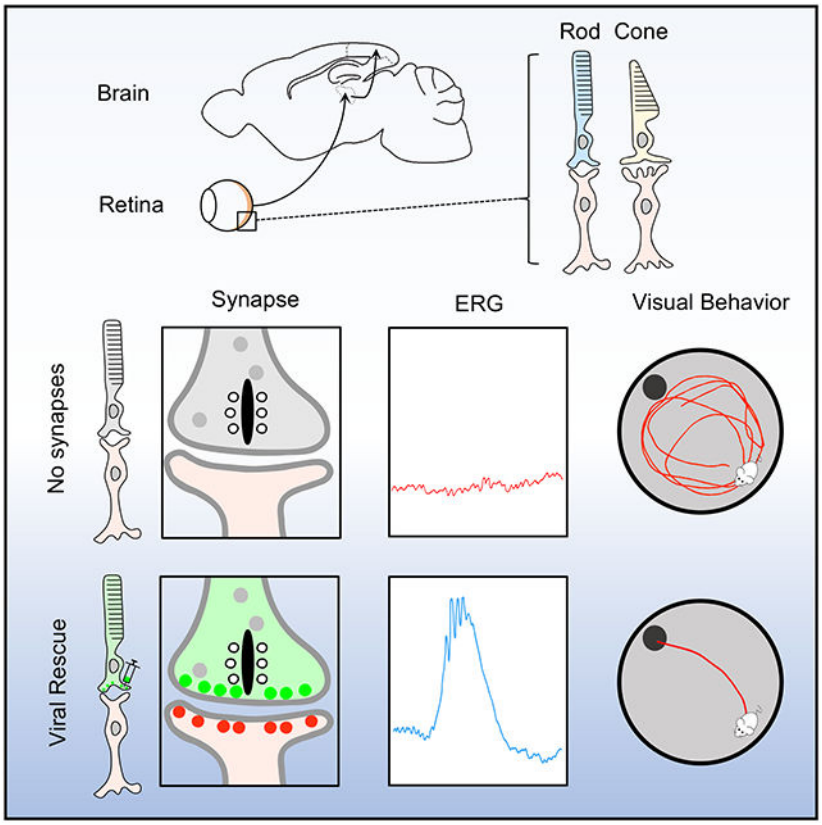

eTOC Blurb

Cao et al. examine the mechanisms that govern post-developmental connectivity of rod photoreceptors into the retinal circuitry. The study reports that rod synapse formation can be restored in adult mice enabling their rod mediated vision at the behavioral level.

Keywords

Vision; retina; synapses; plasticity; critical period; cell adhesion molecules

Introduction

A relationship between form and function has long captivated biologists from many angles. In the nervous system, examining this question is particularly relevant for understanding the development and function of neural circuits. Circuits are formed in a stereotypically programmed fashion with defined anatomical and functional properties [1,2]. Yet, despite this “hard-wiring”, the activity patterns driven by sensory input are required to refine organization of circuits making them suitable for guiding behavior with precision [3,4]. Interestingly, this circuit shaping is thought to be possible only during a specific window in development referred to as the critical period (CP)[5,6]. The absence of the refining input during development leaves circuits poorly suited for powering specific behavioral tasks

and stimulation after closure of the critical period is generally found to be ineffective in correcting these operational deficits [7-13].

Significant progress has been made in defining mechanisms that govern gating of critical periods and circuit plasticity [14-23]. There is also a growing consensus that it has far reaching implications for understanding neuropsychiatric process and development of therapeutic interventions [5,24-27]. However, many fundamental questions related to the extent of plasticity, molecular factors involved and differences in malleability of individual circuits to manipulations outside of the critical period remain open.

There have been significant advances in elucidating anatomy and functional specification of visual circuitry [28,29]. In particular, we now have an exquisitely detailed picture of how vision at the lowest light intensities is orchestrated [30-33]. With the world being dark approximately half of the time, an ability to see at night is paramount for survival of most vertebrate species. This process is enabled by highly sensitive rod photoreceptors [34-37]. To reliably transmit stimuli generated in response to single photons of light, rods must relay their signals via a dedicated high gain channel known as primary rod pathway [38-40]. In this circuit, operating near the absolute visual threshold, rods synaptically communicate with their postsynaptic partners, the rod ON-bipolar neurons [41,42]. Disruption of this process leads to congenital night blindness illustrating that the primary rod pathway is indispensable for a highly stereotypic night vision [43-64]. However, how hard wired and plastic rod photoreceptor synapses are for enabling behaviorally relevant vision is an open question. Answering it will have significant bearing not only for understanding fundamental neurobiology of circuitry development but also for translational efforts aimed at restoring vision lost to degenerative process.

Examining plasticity of the photoreceptor wiring may have implications for understanding CP in the vertebrate visual system, where it was originally defined [9,13]. Complete deprivation from retina inputs during early development leads to profound disorganization of the visual circuit in the brain and inability of animals to rely on vision for guiding behavior following CP closure [7,8,10-12,65,66]. Interestingly, clinical evidence from humans suffering from correctable vision-depriving conditions from early childhood indicates that restoration of visual function could be achieved past CP closure [67]. This suggests capacity for post-developmental plasticity of the higher order visual circuit allowing it to handle visual information when retina inputs were not completely obliterated. However, studies examining the boundaries of CP plasticity in driving behavioral vision with circuit precision have been lacking.

In this work we relied on advanced molecular genetics to manipulate synaptic connectivity of rods, selectively switching their communication on and off post-development while studying the impact on signal propagation along primary rod pathway and vision at the behavioral level. Our results reveal remarkable post-developmental plasticity of physical rod photoreceptor wiring in adult visual system which could be exploited therapeutically.

Results

Cell adhesion mechanisms of mature photoreceptors for maintaining synaptic alignment and transduction of visual signals.

Probing the plasticity of circuit organization and its contribution to behavior requires an ability to molecularly manipulate the configuration of the light input at precise developmental stages without compromising the viability or activity of the photoreceptors and their signaling capacity. In searches for a critical molecular factor for such manipulation, our attention was drawn to a cell adhesion molecule of rods, Elfn1. Its deletion in mice has been shown to selectively and completely abolish synaptic communication of rods without compromising their viability while preserving cone function and transduction of the light signals via secondary pathways [68]. Thus, manipulations with Elfn1 may allow for specific isolation of the primary rod pathway's contribution to vision. To date, however, it was only shown to be required for the assembly of the circuit early in development.

To test the utility of E1fn1 for manipulating circuit configuration post-developmentally, we first probed whether Elfn1 continues to function after development is complete. To enable such studies, two modified *Elfn1* alleles were used. First, we developed a conditional driver line knocking in tamoxifen-sensitive Cre recombinase (CreERT2) under the control of endogenous *Elfn1* promoter (*Elfn1*^{CreERT2}). We confirmed the activity of the Cre recombinase specifically in rods upon induction with tamoxifen by crossing the line with the Ai14 reporter strain (Figure S1). We then crossed it with mice carrying a conditional *Elfn1*^{flx} allele to obtain gene-autonomous conditional *Elfn1*$^{flx/CreERT2}$ mice (cKO). In this model, Elfn1 loss was induced in adult mice (P21) by repeated injections of tamoxifen (Figure 1A). Mice not receiving tamoxifen served as controls and had readily detectable Elfn1 and mGluR6 at rod synapses (Figure 1B). Importantly, treatment with tamoxifen dramatically reduced Elfn1 levels which was accompanied by a severe reduction in mGluR6 accumulation at synapses (Figure 1B,C). Consistent with these observations, we found that transmission of synaptic signals of rods to ON-RBC was nearly abolished as evidenced by blunted ERG b-wave, barely detectable in mice with lowest Elfn1/mGluR6 content (Figure 1D,E). These deficits were specific to rod synaptic transmission and did not impact transduction of the cone generated signals to ON-CBC as photopic b-wave amplitudes in both dark adapted mice (Figure 1F,G) and mice exposed to rod-suppressing light background (Figure 1I,J) were not affected by the tamoxifen treatment. Neither did we notice any deficits in the ability of the photoreceptors to generate a light response as judged by intact a-waves (Figure 1H,K). Together, these results indicate that loss of Elfn1 in fully developed retinas leads to selective disintegration of rod synaptic communication suggestive of the role Elfn1 in synaptic maintenance in mature retinas.

Post-developmental rescue of Elfn1 expression restores synaptic connectivity and transmission of rods.

Having established a role for Elfn1 in the development and maintenance of synaptic connections of rods, we next asked the central question related to the plasticity of rod connectivity and whether its restoration was possible in mature retinas where rods had never been connected to their postsynaptic ON-BC partners. To technically enable these

studies, we generated a conditional rescue allele (*Elfn1*$^{CR/CR}$) by inverting the exon 2 of the *Elfn1* gene relative to its normal endogenous orientation and flanking it with loxP sites to allow Cre-induced restoration of normal gene organization (Figure S2A). We found complete elimination of Elfn1 immunoreactivity in rod synapses of *Elfn1*$^{CR/CR}$ retinas, accompanied by loss of mGluR6, (Figure S2B, C). This was accompanied by predicted loss of rod synaptic transmission as evidenced by complete loss of scotopic ERG b-wave (Figure S2D, E). Thus, our *Elfn1*^{CR} allele is a complete null and phenocopies the effects of the global *Elfn1* KO [68]. Validating the approach, we bred *Elfn1*^{CR} mice with the *Pcdh21*^{Cre} line, a constitutive driver active in photoreceptors (Figure S2A) in order to achieve the developmental conditional rescue of Elfn1 in photoreceptors (pCR). Indeed, we observed that retinas of pCR mice contained both Elfn1 and mGluR6 synaptic puncta (Figure S2B, C). Furthermore, synaptic transmission was also rescued in pCR mice (Figure S2D, E) indicating the general success of genetic rescue strategy of Elfn1 expression and rod synaptic organization early in development.

To test the impact of Elfn1 restoration on synaptic organization after the closure of developmental window we turned to a viral-mediated expression of Cre recombinase in rods of two-month-old *Elfn1*$^{CR/CR}$ mice (Figure 2A, B). Subretinal injection of AAV8-hGRK1-Cre-P2A-GFP led to efficient transduction of photoreceptors and resulted in prominent restoration of synaptic Elfn1 in rods accompanied by re-appearance of mGluR6 (Figure 2C, D) as well as other key synaptic signaling molecules (Figure S3A) at the dendritic tips. Pre-synaptic molecules not affected by Elfn1 elimination were also unaffected by its restoration with AAV-Cre indicating specificity of the effect (Figure S3B).

Importantly, ultrastructural examination revealed that AAV-Cre expression further restored normal morphology of rod synapses: while invaginating rod ON-BC dendrites were absent in control *Elfn1*$^{CR/CR}$, they were quantitatively detectable in rod spherules following AAV-mediated Cre delivery (Figure 2E, F). Overall, these results reveal that Elfn1 re-expression in mature retinas where synaptic contacts of rods had not been developed leads to post-developmental synapse formation and accumulation of receptors mediating the synaptic communication.

We next asked the question whether anatomically restored synapses are functional by evaluating light responses of the retina by ERG. We found that AAV-Cre injected mice showed robust b-waves, albeit lower than in wild-type mice, upon activating rods only with dim scotopic flashes (Figure 2G, H). This was in stark contrast with completely absent scotopic b-waves in control animals lacking Elfn1 (Figure 2G, H). Notably, AAV-mediated Cre expression in rods did not affect the processing of signals by cone photoreceptors and synaptic transmission of cone signals as evidenced by no differences between the groups in either a-waves of b-waves upon photopic stimulation with or without rod suppressing light background (Figure S3C-H). Thus, we conclude that connecting rods into mature circuits after the completion of development permits functional transduction of light evoked signals.

Mice with post-developmentally restored rod wiring fully regain scotopic vision.

An ability to restore functional synaptic connectivity of rods in mature mice allows us to address the central question: can restoration of rod wiring support behavior guided by

vision? We investigated this issue using a water-maze navigational task where animals must rely on vision to locate an escape platform. First, *Elfn1*$^{CR/CR}$ mice were trained to locate a visible escape platform under photopic conditions when mice do not rely on rod inputs for vision (Figure 3A). Mice showed steady improvement in their performance plateauing after 3 days of training when they swam directly to the platform with an average escape latency of 5.47±0.47 s (Figure S4A,B). The same level of performance was observed in *WT* mice with unperturbed visual function (5.41±0.57 s). In control experiments, the platform was hidden and the mice had to locate it by randomly sampling the space without relying on vision. This substantially prolonged the escape latencies with an average of 36.19±2.05 s. Again, this was no different from the performance of the *WT* mice in the same task (30.84±4.67 s). Thus, the difference in escape latencies between visible and hidden platform can serve as a behavioral measure of visual function. Notably, when the mice were evaluated under scotopic conditions requiring the rod pathway to be active, the escape latencies of *Elfn1*$^{CR/CR}$ mice, but not those of *WT,* were no different than those observed for the hidden platform, indicating that at the outset, mice lacking rod synaptic inputs have completely lost visual function in a dim light environment (Figure S4A,B). Next, the animals were split into two cohorts with each receiving either AAV-Cre or control AAV8-hGRK1-GFPvector delivered by subretinal injections (Figure 3A). When mice were evaluated for the behavior four weeks later, we found that all of the AAV-Cre injected animals showed decreased escape latencies under the scotopic conditions (Figure 3B,C). In contrast, mice injected with the AAV-GFP control showed no improvement in their behavior. Both groups performed equally well in a photopic lighting environment (Figure 3F).

Interestingly, we noted significant variability in the extent of the behavioral improvement in AAV-Cre injected group. To understand the nature of this variability we performed ERG on all subjects and noted similar variability in the extent of the b-wave magnitude (Figure 3D). Plotting the amplitudes of scotopic b-waves against the escape latencies in the behavioral task revealed a strong correlation (Figure 3E), indicating that restoration of the visual function is likely limited by the degree of the functional improvement in the synaptic transmission which in turn depends on the efficiency of the AAV transduction in individual mice. Thus, to isolate the impact of reconnecting the rods on vision, we focused on mice with the largest degree of functional rescue, restricting our analysis to mice with ERG b-wave that reached at least 25% of the normally sized response in the model without Elfn1 elimination (as in Figure 1). Analysis of the behavior in these mice revealed complete restoration of visually guided behavior under a scotopic light environment (Figure 3F). Indeed, their visual task performance was equivalent to that of WT mice or to mice evaluated under the photopic conditions. Overall, these results indicate that restoring synaptic inputs of rod photoreceptors fully enables behavioral vision in adult mice which had not previously had any rod-mediated vision.

Recognition of rod synaptic terminals by ON-bipolar dendrites occurs independently from the synapse formation.

Our finding that the formation and function of rod synapses can be readily rescued post-development raises questions about the mechanisms underlying plasticity of the processes involved in aligning the contacts between rods and their synaptic partners, the ON-BC

neurons. To address this, we turned to experiments where we studied the relationship between synapse formation and alignment of rod axons with ON-BC dendrites by cell-cell recognition. First, we analyzed the positioning of the rod synaptic contacts in retinas with misplaced positioning of rod axonal spherules. Normally, rod axons terminate in the outer plexiform layer (OPL) where they meet ON-BC dendrites to make synaptic contacts (Figure 4A,B). However, under certain conditions, rod spherules retract into the outer nuclear layer (ONL) inducing well-documented sprouting of ON-BC dendrites into this area [69-73]. We reasoned that if synapse formation plays a role in this process, Elfn1/mGluR6 pairing would be found at the sites of the ectopic contacts. We used three different models that induce ectopic sprouting: aged retinas, knockout of central metabolic regulator LKB1 and elimination of the active zone protein CAST (Figure 4B). We found similar levels of stochastic ON-BC dendritic sprouting in all of these models (Figure 4B,D). In all of these cases, axons retracted to ONL marked by presynaptic marker PSD95 in ribbons (Figure 4B). Importantly, double-staining experiments revealed that Elfn1 was localized in retracted axonal terminals in direct apposition to postsynaptic receptor mGluR6 at the tips of the sprouting dendritic tips in all models (Figure 4C, D). Thus, trans-synaptic interaction of mGluR6-Elfn1 can occur upon displaced matching of ON-BC dendrites with prematurely terminating axons highlighting the plasticity of the synapse formation process.

Since Elfn1-mGluR6 trans-synaptic contact is essential for establishing the rod to rod-ON-BC synapse, we next asked whether the dendritic sprouting can be prevented by eliminating synapse formation. To address this question, we studied the effect of Elfn1 or mGluR6 loss which both prevent synapse formation on dendritic sprouting in the *CAST*$^{-/-}$ model. We found ectopic sprouting was no different between the retinas with a singular elimination of CAST and when CAST was concurrently eliminated with either Elfn1 or mGluR6 (Figure 4E,F). This indicates that seeking of rod axons by ON-bipolar dendrites and physical matching of both processes occurs independently from the synapse formation driven by trans-synaptic mGluR6-Elfn1 interaction.

Synaptic targeting of Elfn1 is autonomous and independent of synaptic assembly

Given the trans-synaptic nature of interactions involving Elfn1 we next inquired whether its positioning at the axonal terminals of rods depends on the components of the postsynaptic compartment in ON-BC. Our strategy was to systematically delete key components of postsynaptic compartment in mice to study their impact on Elfn1 localization (Figure 5A). Eliminating TRPM1, the principal ion channel that mediates depolarizing response of ON-BC did not affect synaptic targeting of Elfn1 (Figure 5B, S5). Similarly, knockout of RGS proteins RGS7 and RGS11 that constitute the GAP complex that plays an essential role in generating postsynaptic response in ON-BC also failed to affect synaptic accumulation of Elfn1 (Figure 5B, S5). Furthermore, no effect was observed upon deletion of the orphan receptor, GPR179 (Figure 5B), which engages in trans-synaptic contacts with Pikachurin-dystroglycan complex in rod terminals [74].

We previously reported that elimination of mGluR6 compromises the stability of Elfn1 reducing its expression level as assessed by Western blotting [68]. This leaves the question whether Elfn1 is still targeted to synapses in the absence of mGluR6 despite its reduced

expression. To answer this question, we performed a quantitative analysis of Elfn1 distribution in the synaptic photoreceptor layer of retinas lacking mGluR6 (Figure 5C). We found that in *Grm6*$^{-/-}$ retinas, despite the reduction in concentration, Elfn1 could still be concentrated in ribbon synapses (Figure 5C). Thus, the ability of Elfn1 to accumulate at rod synapses is independent from postsynaptic organization and its interaction with mGluR6. Since photoreceptor to ON-BC synapses also fail to form in retinas lacking mGluR6, we further conclude that presynaptic targeting of Elfn1 is independent of physical synapse formation.

Discussion

In this study, we achieve selective post-developmental manipulation of rod photoreceptor synaptic connectivity. With targeted genetic manipulations we were able to disconnect rods from their exclusive synaptic partners (ON-BC neurons) and then to physically reconnect them in mature retinas. This enabled us to address one of the central questions pertaining to plasticity in the organization of the visual circuit- can introduction of highly sensitive retina inputs absent from birth successfully drive visually guided behavior in adult animals? We report that connecting rods in adult mice not only resulted in their physical wiring with ON-bipolar neurons and enabled functional synaptic transmission but also remarkably resulted in emergence of dim light vision not present in the animals at any point before.

The acquisition of visual information first occurs in the retina followed by further processing in the lateral geniculate nucleus (LGN) and visual cortex. Current dogma posits that visual activity and experience play essential roles in visual circuit development. Since Huber and Weisel demonstrated the response of visual cortex neurons to light stimulation was shifted when one eye was deprived of vision in cats during the first few months of life [9,13], this vision-dependent critical period for ocular dominance columns has been extensively studied in various mammalian species [7,8,10-12]. The establishment of synaptic connections is thought to be complete before eye opening and occur independently from light inputs, although dark rearing can block the refinement of retinal ganglion cell (RGC) responses [75,76]. Dark rearing also disrupts cone-mediated but not rod-mediated response [77]. Furthermore, blockage of depolarizing ON-BCs by applying glutamate analogue to developing cat retinas delay the stratification of ON and OFF ganglion cell dendrites [78].

While prior studies manipulated entire visual inputs, we investigated more circuit selective intervention by disconnecting only high sensitivity rod inputs. It is known that rod and cone pathways converge in the retina by the time they reach output neurons: retina ganglion cells [79]. Thus, our results indicate that a generalized pathway, independent of rod photoreceptor activity, may be sufficient for entrainment of higher-order brain structures permitting development of cortical organization with plasticity to then receive additional inputs with distinct characteristics. This in turn enables higher-order vision that guides complex behavioral tasks. These observations give hope to vision restoration approaches for congenital disorders that target adults with gene replacement strategies. Indeed, viral gene transfer studies indicate that propagation of photoreceptor signals could be restored in other models of congenital stationary night blindness featuring synaptic dysfunctions [80-83]. This progress paves the way for asking several exciting questions pertaining to

the organization of the visual circuitry. For example, dissecting the contribution of rod specific rescue in the absence of functioning cones or how central nervous system in higher visual centers handles the post-developmental plasticity of the photoreceptor inputs are important questions. Furthermore, exploring whether viral expression of Elfn1 for its key role in rod photoreceptor communication could be generally beneficial in correcting synaptic deficiencies observed in a variety of models and conditions will be of interest.

Our study also clarifies the mechanistic basis behind the ability of rods to rewire following the completion of retina circuit development. We report that, regardless of physical synapse formation, rod photoreceptor axonal terminals maintain close proximity and likely contacts with the dendrites of the ON-BC. This allows us to conclude that the process of axono-dendritic matching for the photoreceptor-bipolar wiring is independent of the establishment of the synaptic connectivity between these cells. As photoreceptors develop, they send axons that terminate specifically in the outer plexiform layer (OPL) of the retina. Then ON-BCs extend their dendrites initially all the way through the photoreceptor layer followed by their pruning, restricting their terminating points at the OPL [84,85]. Because axonal dendritic matching co-insides with synaptogenesis, it was unclear how these processes interact and whether synapse formation is essential for guiding dendritic processes to axonal terminals.

The identification of Elfn1 as a critical factor for synapse formation provided an excellent opportunity to answer this question. We found that Elfn1 is targeted to axonal terminals independently from the mGluR6-containing postsynaptic complex and elimination of either mGluR6 or Elfn1, while preventing synaptogenesis, had no impact on axono-dendritic pairing between rods and ON-BC. This leads to a conclusion that selective recognition of postsynaptic partners by rod photoreceptors occurs independently from their synapse formation. Several cell adhesion molecules have been identified to facilitate pairing of pre- and postsynaptic neurites and guiding them to the same lamina [86-88]. In the retina, these include repulsive guidance cue semaphorin 6A (Sema6A) and its receptor Plexin A4 (PlexA4) [89-91], cadherin family protein Dscams/Sidekicks [86,87,92,93] and transmembrane proteins MEGF10/11 [94,95]. The identity of the molecular factor(s) mediating matching of photoreceptor and ON-BC processes is currently unknown. Its identification and relationship with synaptogenic Elfn1 function will be of significant interest.

STAR METHODS

RESOURCE AVAILABILITY

Lead contact—Further information and requests for resources and reagents should be directed to and will be fulfilled by the lead contact, Dr. Kirill Martemyanov (kmartemyanov@ufl.edu).

Materials availability—The Mouse lines generated in this study are available upon request from the lead contact.

Data and code availability

- Original data reported in this paper will be shared by the lead contact upon request.

- This paper does not report original code.
- Any additional information required to reanalyze the data reported in this paper is available from the lead contact upon request.

EXPERIMENTAL MODEL AND SUBJECT DETAILS

Trpm1$^{-/-}$, *Rgs7*$^{-/-}$ *Rgs*11$^{-/-}$, *Gpr139*$^{-/-}$, *Lkb1*$^{-/-}$, *Elfn1*$^{-/-}$, *CAST*$^{-/-}$, *Elfn1*$^{flx/flx}$, *Grm6*$^{-/-}$ mouse lines were described previously [68,70,96-103]. Reporter line Ai14 (B6;129S6-Gt(ROSA)26Sor$^{tm14(CAG-tdTomato)Hze}$/J) was obtained from the Jackson Laboratory. *Elfn1*^{CreERT2} mouse was generated by recombination replacing of exon 2 of *Elfn1* gene with CreERT2 cassette. The specificity and efficiency of Cre recombination in *Elfn1*^{CreERT2} lines are evaluated by crossing with Ai14 strain. Conditional targeting of Elfn1 was achieved by flanking exon 2 with LoxP sites (*Elfn1*$^{flx/flx}$). The resulting mice were crossed with *Elfn1*^{CreERT2} line to generate *cKO* strain (*Elfn1*$^{CreERT2/flx}$). The mice carrying the *Elfn1*^{CR} allele are achieved by inverting the exon 2 of *Elfn1* gene relative to their normal endogenous orientation and are flanked with loxP66 and loxP71 sequences inserted in an inverted orientation relative to each other. The resulting mice were crossed with photoreceptor-specific Cre driver line *Pcdh21*^{Cre} [104,105] to produce *Elfn1*$^{CR/CR}$*Pcdh21*^{Cre} strain (*pCR*).

To induce Cre expression, tamoxifen (Sigma, St. Louis, MO), dissolved in ethanol, then mixed with corn oil. The ethanol was removed by evaporator (SAVANT ISS110, Thermo Scientific).75 mg/kg was administered by intraperitoneal injection with a 27 gauge smooth tip needle. Tamoxifen was administered once daily for one five-consecutive day section or three five-consecutive day sections. Mice used in the study were 1–3 months old and were maintained on a diurnal 12 h light/dark cycle. Procedures involving mice strictly followed NIH guidelines and were approved by the Institutional Animal Care and Use Committee at Scripps Florida.

METHOD DETAILS

Antibodies and genetic constructs—Generation of rabbit anti-RGS11[106], sheep anti-TRPM1, sheep anti-mGluR6 and rabbit anti-Elfn1 antibodies were described previously [68,96]. Rabbit anti-$Ca_V1.4$ [73] was a generous gift from Dr. Amy Lee (University of Iowa, IA). Rabbit anti-LRIT3[107] was a generous gift from Dr. Christina Zeits (Institut de la Vision). Commercial antibodies were: mouse anti-CtBP2 (612044, BD Biosciences), mouse anti-PKCα (ab11723; Abcam), rabbit anti-PSD95 (D27E11, Cat# 3450S, Cell Signaling Technology).

Adeno associated virus (AAV8)- based vector containing three surface-exposed proteosomal avoidance mutations (Y447F, Y733F and T494V) was packaged with a construct containing the human rhodopsin kinase 1 (hGRK1) promoter driving Cre recombinase, followed by a P2A cleavage site and green fluorescent protein (GFP)(pTR-hGRK1-Cre-P2A-GFP). Control vectors (packaged in the same capsid) contained hGRK1 driving GFP. Use of the hGRK1 promoter ensures photoreceptor specificity for Cre recombinase and GFP expression [108].

Subretinal Injections—Two-month-old mice were anesthetized by 100 mg/kg Ketamine and 10 mg/kg Xylazine. A small incision in the sclera near the cornea through the skin using the tip of a sharp 30-gauge needle. An injection needle was carefully inserted into the eyeball through the incision to the subretinal space between RPE and retina. 1 μl rAAV virus (5×10^{10}) was slowly injected into the subretinal space. The mice were warmed up by a heat blanket until they recovered from the anesthetic before returned to their mother. ERG was performed five weeks after surgery.

Immunohistochemistry—Dissected eyecups were fixed for 15 min in 4% paraformaldehyde, cryoprotected with 30% sucrose in PBS for 2 h at room temperature, and embedded in optimal cutting temperature medium. Twelve-micron thick frozen sections were cut, mounted onto slides and blocked in PBS with 0.1% Triton X-100 and 10% donkey serum for 1 hour. They then were incubated with the primary antibody in PBS with 0.1% Triton X-100 and 2% donkey serum for at least 1 hour. After four washes with PBS with 0.1% Triton (PT), sections were incubated with fluorophore-conjugated secondary antibodies in PT for 1 h. After four washes, sections were mounted in Fluoromount (Sigma). Images were taken with Zeiss LSM 780/880 confocal microscope. Quantitative analysis of puncta immunofluorescence from confocal images was performed using Metamorph software.

Evaluation of vision by behavioral water maze task—Mouse visual behavior was assessed using a water maze task with a visible escape platform. The method for assessing visual function in this experiment is principled on a Morris water maze [109], and previous reports describing evaluation of mouse vision by a swimming-based task [110]. Mice are natural swimmers, and this task exploits their innate inclination to escape from water to a solid substrate. This task uses an ability of a mouse to see a visible platform with a timed escape from water, as an index of its visual ability. Before testing, mice readily learned to swim to the visible escape-platform and performance usually plateaued at around 10 seconds within 15 trials for all treated groups. Mice that did not learn the task, e.g. performance did not improve or plateau for at least the last 3 or more consecutive trials or had any visible motor deficits were discarded from the experiment. Visually-guided behavior was tested at 100and 0.001 cd/m^2 and timed-performances from 20 trials (4 sessions of 5 trials each) for each mouse at each light-intensity were averaged. Uniform room luminance settings were stably achieved by an engineered adjustable light-source and constantly monitored with a luminance meter LS-100 (Konica Minolta). To be certain that we were measuring the mice's visual ability only and not memory, the platform was placed pseudo-randomly in the water tank and all external visual cues were eliminated.

Electroretinography (ERG)—Electroretinograms were recorded by using the UTA system and a Big-Shot Ganzfeld (LKC Technologies). Mice (6~8 weeks old) were dark-adapted (≥6 h) and prepared for recordings using a dim red light. Mice were anesthetized with an i.p. injection of ketamine and xylazine mixture containing 100 and 10 mg/kg, respectively. All procedures were approved by the Institutional Animal Care and Use Committee at the Scripps Florida Research Institute. The pupil was dilated with 10% phenylephrine hydrochloride (Akorn), followed by the application of 0.5% Tropicamide

(Akorn). Recordings were performed with a gold loop electrode supplemented with contact lenses to keep the eyes immersed in solution. The reference electrode was a stainless steel needle electrode placed subcutaneously in the neck area. The mouse body temperature was maintained at 37 °C by using a heating pad controlled by ATC 1000 temperature controller (World Precision Instruments). ERG signals were sampled at 1 kHz and recorded with 0.3-Hz low-frequency and 300-Hz high-frequency cut-offs.

Full field white flashes were produced by a set of LEDs (duration < 5 ms) for flash strengths ≤2.5 cd· s/m^2 or by a Xenon light source for flashes > 2.5 cd· s/m^2 (flash duration < 5 ms). Given increased mortality of mice lacking Elfn1 undergoing anesthesia and experimental design pairing ERG recordings with behavioral evaluation, ERG responses were elicited only by two flashes at fixed intensities to stimulate rods only (0.001 cd*s/m^2) and all photoreceptors (100 cd*s/m^2). Ten trials were averaged for responses evoked by flashes 0.001 cd*s/m^2, single flash responses were recorded for 100 cd*s/m^2. To allow for recovery, interval times between single flashes were as follows: 5 s for 0.001 cd*s/m^2. Rod-saturating light background of 32 cd/m^2 was administered for recording cone-only ERGs. Ten trials elicited from 100 cd*s/m^2 flashes were averaged at an interval recovery time of 1 second between flashes.

ERG traces were analyzed using the EM LKC Technologies software and Microsoft Excel. The a-wave amplitude was calculated as the value difference between the onset of light flash and the peak of the deflection wave for both dark and light-adapted ERG. The b-wave amplitude was calculated from the bottom of the a-wave response to the peak of the b-wave for both dark and light-adapted ERG.

Electron Microscopy—Eyes were enucleated, cleaned of extra-ocular tissue, and pre-fixed for 15 min in 100 mM cacodylate-buffered half-Karnovsky's fixative containing 2mM calcium chloride. Then the eyecups were hemisected along the vertical meridian and fixed overnight in the same fixative. The specimens were rinsed with cacodylate buffer and postfixed in 2% osmium tetroxide in water for 1 hour, en-block stained with 1% uranyl acetate for 25 minutes, then gradually dehydrated in an increasing ethanol and acetone series (30–100%), and embedded in Durcupan ACM resin (Sigma Aldrich). Blocks were cut with 70 nm-thickness and were stained with 3% uranyl acetate and 0.5% lead citrate. Sections were examined in a Tecnai G2 spirit BioTwin (Thermo Fisher Scientific, Waltman, MA, United States) transmission electron microscope at 100 kV accelerating voltage. Images were captured with a Veleta CCD camera (Olympus, Tokyo, Japan) operated by TIA software (Thermo Fisher Scientific, Waltman, MA, United States).

QUANTIFICATION AND STATISTICAL ANALYSIS

Statistics were performed using GraphPad Prism 9 software. Unless otherwise noted, at least three independent samples were used for statistical comparisons. Statistical significance on bar graphs and box plots was expressed as * P<0.05, ** P<0.01, *** P<0.001, and **** P<0.0001. Not significant (n.s.) was indicated where appropriate. Data were expressed as mean ± SEM with all data points provided representing n.

Supplementary Material

Refer to Web version on PubMed Central for supplementary material.

Acknowledgements

We thank Ms. Natalia Martemyanova for performing the genetic crosses needed to obtain mice utilized in these studies. We thank Light Microscopy Core in Max Planck Florida Institute for Neuroscience for supporting image acquisition. This work was supported by NIH grants EY018139 and EY028033 (KAM), EY024280 (SEB), EY030458 and EY02798 (MAS), and by Japan Society for the Promotion of Science KAKENHI grant15H04272 (TO).

Inclusion and diversity Statement

We support inclusive, diverse, and equitable conduct of research.

References

1. Bargmann CI & Marder E From the connectome to brain function. Nat Methods 10, 483–490 (2013). [PubMed: 23866325]
2. Tau GZ & Peterson BS Normal development of brain circuits. Neuropsychopharmacology 35, 147–168, doi:10.1038/npp.2009.115 (2010). [PubMed: 19794405]
3. Hooks BM & Chen C Circuitry Underlying Experience-Dependent Plasticity in the Mouse Visual System. Neuron 106, 21–36, doi:10.1016/j.neuron.2020.01.031 (2020). [PubMed: 32272065]
4. Sengpiel F & Kind PC The role of activity in development of the visual system. Curr Biol 12, R818–826, doi:10.1016/s0960-9822(02)01318-0 (2002). [PubMed: 12477410]
5. Marin O Developmental timing and critical windows for the treatment of psychiatric disorders. Nat Med 22, 1229–1238, doi:10.1038/nm.4225 (2016). [PubMed: 27783067]
6. Hooks BM & Chen C Critical periods in the visual system: changing views for a model of experience-dependent plasticity. Neuron 56, 312–326, doi:10.1016/j.neuron.2007.10.003 (2007). [PubMed: 17964248]
7. Fagiolini M, Pizzorusso T, Berardi N, Domenici L & Maffei L Functional postnatal development of the rat primary visual cortex and the role of visual experience: dark rearing and monocular deprivation. Vision Res 34, 709–720, doi:10.1016/0042-6989(94)90210-0 (1994). [PubMed: 8160387]
8. Gordon JA & Stryker MP Experience-dependent plasticity of binocular responses in the primary visual cortex of the mouse. J Neurosci 16, 3274–3286 (1996). [PubMed: 8627365]
9. Hubel DH & Wiesel TN The period of susceptibility to the physiological effects of unilateral eye closure in kittens. J Physiol 206, 419–436, doi:10.1113/jphysiol.1970.sp009022 (1970). [PubMed: 5498493]
10. Hubel DH, Wiesel TN & LeVay S Plasticity of ocular dominance columns in monkey striate cortex. Philos Trans R Soc Lond B Biol Sci 278, 377–409, doi:10.1098/rstb.1977.0050 (1977). [PubMed: 19791]
11. Issa NP, Trachtenberg JT, Chapman B, Zahs KR & Stryker MP The critical period for ocular dominance plasticity in the Ferret's visual cortex. J Neurosci 19, 6965–6978 (1999). [PubMed: 10436053]
12. LeVay S, Wiesel TN & Hubel DH The development of ocular dominance columns in normal and visually deprived monkeys. J Comp Neurol 191, 1–51, doi:10.1002/cne.901910102 (1980). [PubMed: 6772696]
13. Wiesel TN & Hubel DH Single-Cell Responses in Striate Cortex of Kittens Deprived of Vision in One Eye. J Neurophysiol 26, 1003–1017, doi:10.1152/jn.1963.26.6.1003 (1963). [PubMed: 14084161]

14. Desai NS, Cudmore RH, Nelson SB & Turrigiano GG Critical periods for experience-dependent synaptic scaling in visual cortex. Nat Neurosci 5, 783–789, doi:10.1038/nn878 (2002). [PubMed: 12080341]
15. Goel A & Lee HK Persistence of experience-induced homeostatic synaptic plasticity through adulthood in superficial layers of mouse visual cortex. J Neurosci 27, 6692–6700, doi:10.1523/JNEUROSCI.5038-06.2007 (2007). [PubMed: 17581956]
16. Maffei A, Nelson SB & Turrigiano GG Selective reconfiguration of layer 4 visual cortical circuitry by visual deprivation. Nat Neurosci 7, 1353–1359, doi:10.1038/nn1351 (2004). [PubMed: 15543139]
17. Liu S, Rao Y & Daw N Roles of protein kinase A and protein kinase G in synaptic plasticity in the visual cortex. Cereb Cortex 13, 864–869, doi:10.1093/cercor/13.8.864 (2003). [PubMed: 12853373]
18. Bear MF, Kleinschmidt A, Gu QA & Singer W Disruption of experience-dependent synaptic modifications in striate cortex by infusion of an NMDA receptor antagonist. J Neurosci 10, 909–925 (1990). [PubMed: 1969466]
19. Beaver CJ, Ji Q, Fischer QS & Daw NW Cyclic AMP-dependent protein kinase mediates ocular dominance shifts in cat visual cortex. Nat Neurosci 4, 159–163, doi:10.1038/83985 (2001). [PubMed: 11175876]
20. Rao Y et al. Reduced ocular dominance plasticity and long-term potentiation in the developing visual cortex of protein kinase A RII alpha mutant mice. Eur J Neurosci 20, 837–842, doi:10.1111/j.1460-9568.2004.03499.x (2004). [PubMed: 15255994]
21. Maffei A, Nataraj K, Nelson SB & Turrigiano GG Potentiation of cortical inhibition by visual deprivation. Nature 443, 81–84, doi:10.1038/nature05079 (2006). [PubMed: 16929304]
22. Tropea D et al. Gene expression changes and molecular pathways mediating activity-dependent plasticity in visual cortex. Nat Neurosci 9, 660–668, doi:10.1038/nn1689 (2006). [PubMed: 16633343]
23. Majdan M & Shatz CJ Effects of visual experience on activity-dependent gene regulation in cortex. Nat Neurosci 9, 650–659, doi:10.1038/nn1674 (2006). [PubMed: 16582906]
24. Millan MJ et al. Altering the course of schizophrenia: progress and perspectives. Nat Rev Drug Discov 15, 485–515, doi:10.1038/nrd.2016.28 (2016). [PubMed: 26939910]
25. Kalia A et al. Development of pattern vision following early and extended blindness. Proc Natl Acad Sci U S A 111, 2035–2039, doi:10.1073/pnas.1311041111 (2014). [PubMed: 24449865]
26. Veenstra-VanderWeele J & Warren Z Intervention in the context of development: pathways toward new treatments. Neuropsychopharmacology 40, 225–237, doi:10.1038/npp.2014.232 (2015). [PubMed: 25182180]
27. Hubener M & Bonhoeffer T Neuronal plasticity: beyond the critical period. Cell 159, 727–737, doi:10.1016/j.cell.2014.10.035 (2014). [PubMed: 25417151]
28. Prasad S & Galetta SL Anatomy and physiology of the afferent visual system. Handb Clin Neurol 102, 3–19, doi:10.1016/B978-0-444-52903-9.00007-8 (2011). [PubMed: 21601061]
29. Bence M & Levelt CN Structural plasticity in the developing visual system. Prog Brain Res 147, 125–139, doi:10.1016/S0079-6123(04)47010-1 (2005). [PubMed: 15581702]
30. Burns ME & Arshavsky VY Beyond counting photons: trials and trends in vertebrate visual transduction. Neuron 48, 387–401 (2005). [PubMed: 16269358]
31. Burger CA, Jiang D, Mackin RD & Samuel MA Development and maintenance of vision's first synapse. Dev Biol 476, 218–239, doi:10.1016/j.ydbio.2021.04.001 (2021). [PubMed: 33848537]
32. Gregg RG, Ray TA, Hasan N, McCall MA & Peachey NS in G Protein Signaling Mechanisms in the Retina (eds Martemyanov Kirill A. & Sampath Alapakkam P.) 67–79 (Springer New York, 2014).
33. Vardi N & Dhingra A in G Protein Signaling Mechanisms in the Retina (eds Martemyanov Kirill A. & Sampath Alapakkam P.) 81–97 (Springer New York, 2014).
34. Schneeweis DM & Schnapf JL Photovoltage of rods and cones in the macaque retina. Science 268, 1053–1056, doi:10.1126/science.7754386 (1995). [PubMed: 7754386]
35. Tamura T, Nakatani K & Yau KW Calcium feedback and sensitivity regulation in primate rods. J Gen Physiol 98, 95–130, doi:10.1085/jgp.98.1.95 (1991). [PubMed: 1719127]

36. Rieke F & Baylor DA Origin of reproducibility in the responses of retinal rods to single photons. Biophys J 75, 1836–1857, doi:10.1016/S0006-3495(98)77625-8 (1998). [PubMed: 9746525]
37. Rieke F Mechanisms of single-photon detection in rod photoreceptors. Methods Enzymol 316, 186–202, doi:10.1016/s0076-6879(00)16724-2 (2000). [PubMed: 10800676]
38. Bloomfield SA & Dacheux RF Rod vision: pathways and processing in the mammalian retina. Prog Retin Eye Res 20, 351–384, doi:10.1016/s1350-9462(00)00031-8 (2001). [PubMed: 11286897]
39. Sharpe LT & Stockman A Rod pathways: the importance of seeing nothing. Trends Neurosci 22, 497–504 (1999). [PubMed: 10529817]
40. Dacheux RF & Raviola E The rod pathway in the rabbit retina: a depolarizing bipolar and amacrine cell. J Neurosci 6, 331–345 (1986). [PubMed: 3950701]
41. Taylor WR & Smith RG Transmission of scotopic signals from the rod to rod-bipolar cell in the mammalian retina. Vision Res 44, 3269–3276 (2004). [PubMed: 15535994]
42. DeVries SH & Baylor DA Synaptic circuitry of the retina and olfactory bulb. Cell 72 Suppl, 139–149, doi:10.1016/s0092-8674(05)80033-9 (1993). [PubMed: 8428375]
43. Zeitz C, Robson AG & Audo I Congenital stationary night blindness: an analysis and update of genotype-phenotype correlations and pathogenic mechanisms. Progress in retinal and eye research 45, 58–110, doi:10.1016/j.preteyeres.2014.09.001 (2015). [PubMed: 25307992]
44. Gal A, Orth U, Baehr W, Schwinger E & Rosenberg T Heterozygous missense mutation in the rod cGMP phosphodiesterase beta-subunit gene in autosomal dominant stationary night blindness. Nat Genet 7, 64–68, doi:10.1038/ng0594-64 (1994). [PubMed: 8075643]
45. Bech-Hansen NT et al. Loss-of-function mutations in a calcium-channel alpha1-subunit gene in Xp11.23 cause incomplete X-linked congenital stationary night blindness. Nat Genet 19, 264–267, doi:10.1038/947 (1998). [PubMed: 9662400]
46. Strom TM et al. An L-type calcium-channel gene mutated in incomplete X-linked congenital stationary night blindness. Nat Genet 19, 260–263, doi:10.1038/940 (1998). [PubMed: 9662399]
47. Bech-Hansen NT et al. Mutations in NYX, encoding the leucine-rich proteoglycan nyctalopin, cause X-linked complete congenital stationary night blindness. Nat Genet 26, 319–323, doi:10.1038/81619 (2000). [PubMed: 11062471]
48. Audo I et al. Whole-exome sequencing identifies mutations in GPR179 leading to autosomal-recessive complete congenital stationary night blindness. Am J Hum Genet 90, 321–330, doi:10.1016/j.ajhg.2011.12.007 (2012). [PubMed: 22325361]
49. Audo I et al. TRPM1 is mutated in patients with autosomal-recessive complete congenital stationary night blindness. Am J Hum Genet 85, 720–729, doi:10.1016/j.ajhg.2009.10.013 (2009). [PubMed: 19896113]
50. Bijveld MM et al. Genotype and phenotype of 101 dutch patients with congenital stationary night blindness. Ophthalmology 120, 2072–2081, doi:10.1016/j.ophtha.2013.03.002 (2013). [PubMed: 23714322]
51. Devi S et al. Metabotropic glutamate receptor 6 signaling enhances TRPM1 calcium channel function and increases melanin content in human melanocytes. Pigment Cell Melanoma Res 26, 348–356, doi:10.1111/pcmr.12083 (2013). [PubMed: 23452348]
52. Dryja TP et al. Night blindness and abnormal cone electroretinogram ON responses in patients with mutations in the GRM6 gene encoding mGluR6. Proc Natl Acad Sci U S A 102, 4884–4889, doi:0501233102 [pii] 10.1073/pnas.0501233102 (2005). [PubMed: 15781871]
53. Jacobi FK et al. Phenotypic expression of the complete type of X-linked congenital stationary night blindness in patients with different mutations in the NYX gene. Graefes Arch Clin Exp Ophthalmol 240, 822–828, doi:10.1007/s00417-002-0562-z (2002). [PubMed: 12397430]
54. Leroy BP et al. A common NYX mutation in Flemish patients with X linked CSNB. Br J Ophthalmol 93, 692–696, doi:bjo.2008.143727 [pii] 10.1136/bjo.2008.143727 (2009). [PubMed: 18617546]
55. Li Z et al. Recessive mutations of the gene TRPM1 abrogate ON bipolar cell function and cause complete congenital stationary night blindness in humans. Am J Hum Genet 85, 711–719, doi:10.1016/j.ajhg.2009.10.003 (2009). [PubMed: 19878917]

56. O'Connor E et al. Congenital stationary night blindness associated with mutations in GRM6 encoding glutamate receptor MGluR6. Br J Ophthalmol 90, 653–654, doi:90/5/653 [pii] 10.1136/bjo.2005.086678 (2006). [PubMed: 16622103]
57. Pusch CM et al. The complete form of X-linked congenital stationary night blindness is caused by mutations in a gene encoding a leucine-rich repeat protein. Nat Genet 26, 324–327, doi:10.1038/81627 (2000). [PubMed: 11062472]
58. Scholl HP et al. Slow and fast rod ERG pathways in patients with X-linked complete stationary night blindness carrying mutations in the NYX gene. Invest Ophthalmol Vis Sci 42, 2728–2736 (2001). [PubMed: 11581222]
59. Sergouniotis PI et al. Retinal structure, function, and molecular pathologic features in gyrate atrophy. Ophthalmology 119, 596–605, doi:10.1016/j.ophtha.2011.09.017 (2012). [PubMed: 22182799]
60. van Genderen MM et al. Mutations in TRPM1 are a common cause of complete congenital stationary night blindness. Am J Hum Genet 85, 730–736, doi:10.1016/j.ajhg.2009.10.012 (2009). [PubMed: 19896109]
61. Xu X et al. Sequence variations of GRM6 in patients with high myopia. Molecular vision 15, 2094–2100 (2009). [PubMed: 19862333]
62. Zeitz C et al. Mutations in GRM6 cause autosomal recessive congenital stationary night blindness with a distinctive scotopic 15-Hz flicker electroretinogram. Invest Ophthalmol Vis Sci 46, 4328–4335, doi:10.1167/iovs.05-0526 (2005). [PubMed: 16249515]
63. Zeitz C et al. Novel mutations in CACNA1F and NYX in Dutch families with X-linked congenital stationary night blindness. Mol Vis 11, 179–183 (2005). [PubMed: 15761389]
64. Zeitz C et al. Whole-exome sequencing identifies LRIT3 mutations as a cause of autosomal-recessive complete congenital stationary night blindness. Am J Hum Genet 92, 67–75, doi:10.1016/j.ajhg.2012.10.023 (2013). [PubMed: 23246293]
65. Harwerth RS, Smith EL 3rd, Crawford ML & von Noorden GK Behavioral studies of the sensitive periods of development of visual functions in monkeys. Behav Brain Res 41, 179–198, doi:10.1016/0166-4328(90)90107-p (1990). [PubMed: 2288671]
66. Emerson VF, Chalupa LM, Thompson ID & Talbot RJ Behavioural, physiological, and anatomical consequences of monocular deprivation in the golden hamster (Mesocricetus auratus). Exp Brain Res 45, 168–178, doi:10.1007/BF00235776 (1982). [PubMed: 7056323]
67. Scheiman MM et al. Randomized trial of treatment of amblyopia in children aged 7 to 17 years. Arch Ophthalmol 123, 437–447, doi:10.1001/archopht.123.4.437 (2005). [PubMed: 15824215]
68. Cao Y et al. Mechanism for Selective Synaptic Wiring of Rod Photoreceptors into the Retinal Circuitry and Its Role in Vision. Neuron 87, 1248–1260, doi:10.1016/j.neuron.2015.09.002 (2015). [PubMed: 26402607]
69. tom Dieck S et al. Deletion of the presynaptic scaffold CAST reduces active zone size in rod photoreceptors and impairs visual processing. J Neurosci 32, 12192–12203, doi:10.1523/JNEUROSCI.0752-12.2012 (2012). [PubMed: 22933801]
70. Samuel MA et al. LKB1 and AMPK regulate synaptic remodeling in old age. Nat Neurosci 17, 1190–1197, doi:10.1038/nn.3772 (2014). [PubMed: 25086610]
71. Zabouri N & Haverkamp S Calcium channel-dependent molecular maturation of photoreceptor synapses. PLoS One 8, e63853, doi:10.1371/journal.pone.0063853 (2013). [PubMed: 23675510]
72. Mansergh F et al. Mutation of the calcium channel gene Cacna1f disrupts calcium signaling, synaptic transmission and cellular organization in mouse retina. Hum Mol Genet 14, 3035–3046, doi:10.1093/hmg/ddi336 (2005). [PubMed: 16155113]
73. Liu X et al. Dysregulation of Ca(v)1.4 channels disrupts the maturation of photoreceptor synaptic ribbons in congenital stationary night blindness type 2. Channels 7, 514–523, doi:10.4161/chan.26376 (2013). [PubMed: 24064553]
74. Orlandi C et al. Transsynaptic Binding of Orphan Receptor GPR179 to Dystroglycan-Pikachurin Complex Is Essential for the Synaptic Organization of Photoreceptors. Cell Rep 25, 130–145 e135, doi:10.1016/j.celrep.2018.08.068 (2018). [PubMed: 30282023]

75. Tian N & Copenhagen DR Visual stimulation is required for refinement of ON and OFF pathways in postnatal retina. Neuron 39, 85–96, doi:10.1016/s0896-6273(03)00389-1 (2003). [PubMed: 12848934]
76. Di Marco S, Nguyen VA, Bisti S & Protti DA Permanent functional reorganization of retinal circuits induced by early long-term visual deprivation. J Neurosci 29, 13691–13701, doi:10.1523/JNEUROSCI.3854-09.2009 (2009). [PubMed: 19864581]
77. Dunn FA, Della Santina L, Parker ED & Wong RO Sensory experience shapes the development of the visual system's first synapse. Neuron 80, 1159–1166, doi:10.1016/j.neuron.2013.09.024 (2013). [PubMed: 24314727]
78. Bodnarenko SR & Chalupa LM Stratification of ON and OFF ganglion cell dendrites depends on glutamate-mediated afferent activity in the developing retina. Nature 364, 144–146, doi:10.1038/364144a0 (1993). [PubMed: 8100613]
79. Zhang C, Kolodkin AL, Wong RO & James RE Establishing Wiring Specificity in Visual System Circuits: From the Retina to the Brain. Annu Rev Neurosci 40, 395–424, doi:10.1146/annurev-neuro-072116-031607 (2017). [PubMed: 28460185]
80. Hasan N et al. Presynaptic Expression of LRIT3 Transsynaptically Organizes the Postsynaptic Glutamate Signaling Complex Containing TRPM1. Cell Rep 27, 3107–3116 e3103, doi:10.1016/j.celrep.2019.05.056 (2019). [PubMed: 31189098]
81. Varin J et al. Substantial restoration of night vision in adult mice with congenital stationary night blindness. Mol Ther Methods Clin Dev 22, 15–25, doi:10.1016/j.omtm.2021.05.008 (2021). [PubMed: 34401402]
82. Miyadera K et al. Targeting ON-bipolar cells by AAV gene therapy stably reverses LRIT3-congenital stationary night blindness. Proc Natl Acad Sci U S A 119, e2117038119, doi:10.1073/pnas.2117038119 (2022). [PubMed: 35316139]
83. Scalabrino ML et al. Intravitreal delivery of a novel AAV vector targets ON bipolar cells and restores visual function in a mouse model of complete congenital stationary night blindness. Hum Mol Genet 24, 6229–6239, doi:10.1093/hmg/ddv341 (2015). [PubMed: 26310623]
84. Morgan JL, Dhingra A, Vardi N & Wong RO Axons and dendrites originate from neuroepithelial-like processes of retinal bipolar cells. Nat Neurosci 9, 85–92 (2006). [PubMed: 16341211]
85. Reese BE Developmental plasticity of photoreceptors. Progress in brain research 144, 3–19, doi:10.1016/s0079-6123(03)14401-9 (2004). [PubMed: 14650837]
86. Yamagata M & Sanes JR Dscam and Sidekick proteins direct lamina-specific synaptic connections in vertebrate retina. Nature 451, 465–469, doi:10.1038/nature06469 (2008). [PubMed: 18216854]
87. Yamagata M, Weiner JA & Sanes JR Sidekicks: synaptic adhesion molecules that promote lamina-specific connectivity in the retina. Cell 110, 649–660, doi:10.1016/s0092-8674(02)00910-8 (2002). [PubMed: 12230981]
88. Xiao T et al. Assembly of lamina-specific neuronal connections by slit bound to type IV collagen. Cell 146, 164–176, doi:10.1016/j.cell.2011.06.016 (2011). [PubMed: 21729787]
89. Matsuoka RL et al. Transmembrane semaphorin signalling controls laminar stratification in the mammalian retina. Nature 470, 259–263, doi:10.1038/nature09675 (2011). [PubMed: 21270798]
90. Suto F et al. Interactions between plexin-A2, plexin-A4, and semaphorin 6A control lamina-restricted projection of hippocampal mossy fibers. Neuron 53, 535–547, doi:10.1016/j.neuron.2007.01.028 (2007). [PubMed: 17296555]
91. Suto F et al. Plexin-a4 mediates axon-repulsive activities of both secreted and transmembrane semaphorins and plays roles in nerve fiber guidance. J Neurosci 25, 3628–3637, doi:10.1523/JNEUROSCI.4480-04.2005 (2005). [PubMed: 15814794]
92. Fuerst PG, Koizumi A, Masland RH & Burgess RW Neurite arborization and mosaic spacing in the mouse retina require DSCAM. Nature 451, 470–474, doi:10.1038/nature06514 (2008). [PubMed: 18216855]
93. Fuerst PG et al. DSCAM and DSCAML1 function in self-avoidance in multiple cell types in the developing mouse retina. Neuron 64, 484–497, doi:10.1016/j.neuron.2009.09.027 (2009). [PubMed: 19945391]

94. Kay JN, Chu MW & Sanes JR MEGF10 and MEGF11 mediate homotypic interactions required for mosaic spacing of retinal neurons. Nature 483, 465–469, doi:10.1038/nature10877 (2012). [PubMed: 22407321]

95. Ray TA et al. Formation of retinal direction-selective circuitry initiated by starburst amacrine cell homotypic contact. Elife 7, doi:10.7554/eLife.34241 (2018).

96. Cao Y, Posokhova E & Martemyanov KA TRPM1 forms complexes with nyctalopin in vivo and accumulates in postsynaptic compartment of ON-bipolar neurons in mGluR6-dependent manner. J Neurosci 31, 11521–11526, doi:10.1523/JNEUROSCI.1682-11.2011 (2011). [PubMed: 21832182]

97. Cao Y et al. Regulators of G protein signaling RGS7 and RGS11 determine the onset of the light response in ON bipolar neurons. Proc Natl Acad Sci U S A 109, 7905–7910, doi:10.1073/pnas.1202332109 (2012). [PubMed: 22547806]

98. Hagiwara A et al. Cytomatrix proteins CAST and ELKS regulate retinal photoreceptor development and maintenance. J Cell Biol 217, 3993–4006, doi:10.1083/jcb.201704076 (2018). [PubMed: 30190286]

99. Peachey NS et al. GPR179 is required for depolarizing bipolar cell function and is mutated in autosomal-recessive complete congenital stationary night blindness. Am J Hum Genet 90, 331–339, doi:10.1016/j.ajhg.2011.12.006 (2012). [PubMed: 22325362]

100. Cao Y et al. Interplay between cell-adhesion molecules governs synaptic wiring of cone photoreceptors. Proc Natl Acad Sci U S A 117, 23914–23924, doi:10.1073/pnas.2009940117 (2020). [PubMed: 32879010]

101. Neuille M et al. Lrit3 deficient mouse (nob6): a novel model of complete congenital stationary night blindness (cCSNB). PLoS One 9, e90342, doi:10.1371/journal.pone.0090342 (2014). [PubMed: 24598786]

102. Peachey NS et al. GPR179 Is Required for Depolarizing Bipolar Cell Function and Is Mutated in Autosomal-Recessive Complete Congenital Stationary Night Blindness. Am J Hum Genet 90, 331–339, doi:10.1016/j.ajhg.2011.12.006 (2012). [PubMed: 22325362]

103. Shen Y et al. A transient receptor potential-like channel mediates synaptic transmission in rod bipolar cells. J Neurosci 29, 6088–6093, doi:29/19/6088 [pii] 10.1523/JNEUROSCI.0132-09.2009 (2009). [PubMed: 19439586]

104. Rattner A et al. A photoreceptor-specific cadherin is essential for the structural integrity of the outer segment and for photoreceptor survival. Neuron 32, 775–786, doi:10.1016/s0896-6273(01)00531-1 (2001). [PubMed: 11738025]

105. Boland MJ et al. Adult mice generated from induced pluripotent stem cells. Nature 461, 91–94, doi:10.1038/nature08310 (2009). [PubMed: 19672243]

106. Cao Y et al. Retina-specific GTPase accelerator RGS11/G beta 5S/R9AP is a constitutive heterotrimer selectively targeted to mGluR6 in ON-bipolar neurons. J Neurosci 29, 9301–9313, doi:29/29/9301 [pii] 10.1523/JNEUROSCI.1367-09.2009 (2009). [PubMed: 19625520]

107. Neuille M et al. LRIT3 is essential to localize TRPM1 to the dendritic tips of depolarizing bipolar cells and may play a role in cone synapse formation. Eur J Neurosci 42, 1966–1975, doi:10.1111/ejn.12959 (2015). [PubMed: 25997951]

108. Alexander JJ et al. Restoration of cone vision in a mouse model of achromatopsia. Nat Med 13, 685–687, doi:10.1038/nm1596 (2007). [PubMed: 17515894]

109. Morris R Developments of a water-maze procedure for studying spatial learning in the rat. J Neurosci Methods 11, 47–60 (1984). [PubMed: 6471907]

110. Prusky GT, West PW & Douglas RM Behavioral assessment of visual acuity in mice and rats. Vision Res 40, 2201–2209 (2000). [PubMed: 10878281]

Highlights

- Cell adhesion molecule ELFN1 is essential for maintenance of rod synapses
- Reactivation of ELFN1 expression in adult mice allows rods to form synapses
- Post-developmentally rescued rod synapses are functional
- Mice gain dim light vision upon restoration of rod connectivity in adult retinas

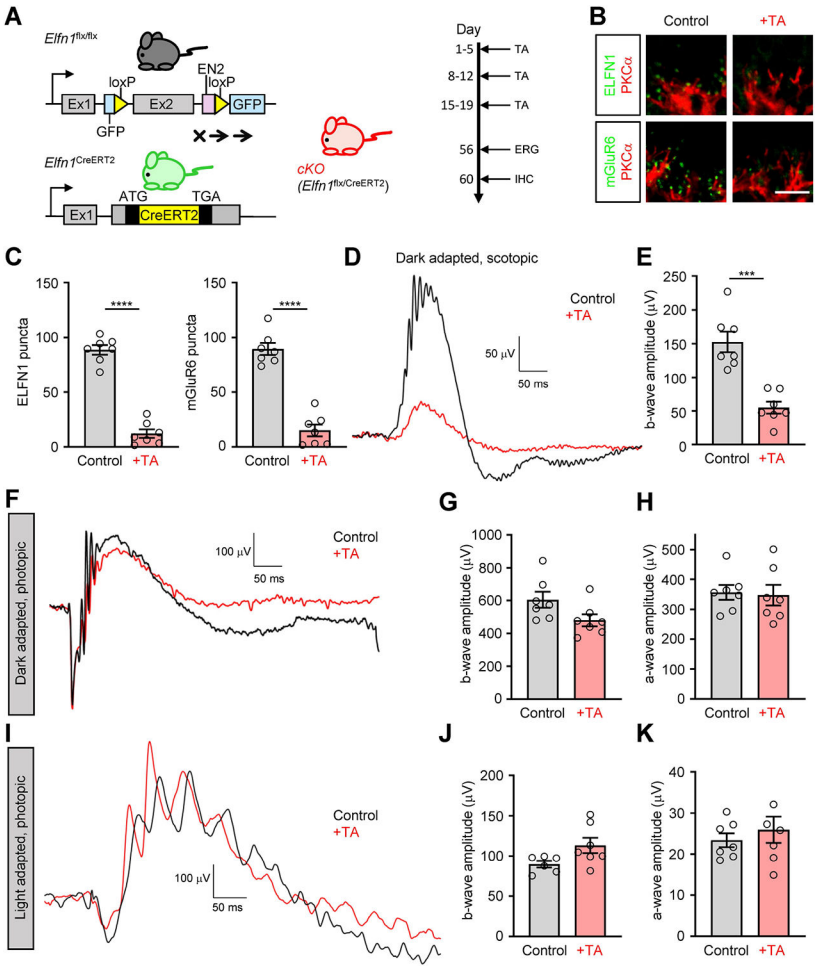

Figure 1. Analysis of post-developmental elimination of Elfn1

(A) Schematic of the strategy for conditional elimination of *Elfn1* in the retina. A conditional knockout allele for *Elfn1* (*Elfn1*$^{flx/flx}$) was generated by flanking exon 2 with loxP sites. *Elfn1*$^{flx/flx}$ mice were crossed with a tamoxifen-inducible Cre strain *Elfn1*^{CreER2} under the the control of endogenous *Elfn1* promoter to generate conditional *Elfn1*$^{flx/CreER2}$ (*cKO*) mice. The 2-month-old *cKO* mice were administered tamoxifen (TA) for three five-day injections to induce ELFN1 loss. One-month post-administration, electroretinograms were recorded, then immunohistochemistry analyses were performed. TA, tamoxifen.

(B) Elfn1 and mGluR6 localization in rods of *cKO* mice. Retina cross-sections were double-immunostained with antibodies against Elfn1(green) or mGluR6 (green) with rod ON-BC marker PKCα (red) (Scale bar, 5 μm.)

(C) Quantification of Elfn1 and mGluR6 in *cKO* mice. Synaptic puncta were counted and averaged from six images per retina collected from seven separate mice in each condition.

(D) Analysis of rod synaptic transmission in *cKO* mice by ERG. Representative traces of responses to a scotopic flash of 0.001 cd*s/m^2 (~0. 6R* per rod) are shown.

(E) Quantification of b-wave ERG amplitudes in *cKO* mice treated with or without tamoxifen under scotopic conditions.

(F) Representative ERG traces to a photopic flash of 100 cd*s/m^2 (~58,000 R*/rod) to activate both rod and cone pathways.

(G) Quantification of b-wave ERG amplitudes in *cKO* mice treated with or without tamoxifen under photopic conditions.
(H) Quantification of a-wave ERG amplitudes in *cKO* mice treated with or without tamoxifen under photopic conditions.
(I) Representative ERG traces to a photopic flash of 100 cd*s/m^2 (~58,000 R*/rod) under a 32 cd*s/ m^2 (~18,500 R*/rod/s) light background to activate the cone pathway only.
(J) Quantification of b-wave ERG amplitudes in *cKO* mice treated with or without tamoxifen under light-adapted photopic conditions.
(K) Quantification of a-wave ERG amplitudes in *cKO* mice treated with or without tamoxifen under light-adapted photopic conditions. Data are represented as mean ± SEM. n=7, ***P < 0.001, ****P < 0.0001, unpaired t-test.
See also Figure S1.

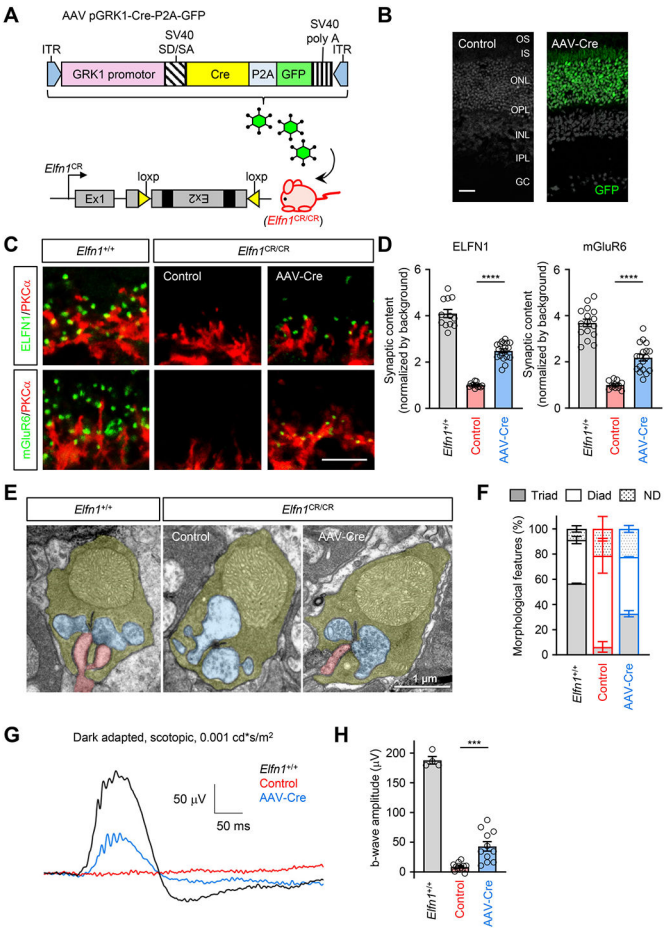

Figure 2. Analysis of post-developmental rescue of Elfn1

(A) Schematic illustration of the strategy for the conditional rescue of *Elfn1* in the retina. The mice carrying the conditional rescue *Elfn1* allele (*Elfn1*$^{CR/CR}$) are obtained by inverting the exon 2 of the *Elfn1* gene relative to their normal endogenous orientation and are flanked with loxP66 and loxP71 sequences inserted in an inverted orientation relative to each other. The restoration of Elfn1 is achieved by subretinal injection of rAAV using human rhodopsin kinase 1 promoter construct to provide photoreceptor specificity for Cre recombinase expression. ITR, inverted terminal repeat; GRK1 promotor, human rhodopsin kinase 1 promoter; SV40 SD/SA, SV40 splice donor/splice acceptor.

(B) Retina cross-section showing GFP induction specifically in the photoreceptor. OS, outer segment; IS, inner segment; ONL, outer nuclear layer; OPL, outer plexiform layer; INL, inner nuclear layer; IPL, inner plexiform layer; GC, ganglion cells. (Scale bar, 25 µm.)

(C) Analysis of the effect of Elfn1 restoration on synaptic content of mGluR6 in rod terminals. Retina cross-sections were double-immunostained with antibodies against Elfn1 (green) or mGluR6 (green) and rod ON-BC marker PKCα (red). Scale bar, 5 µm.

(D) Quantification of Elfn1 and mGluR6 content in rod ON-BC synapses. Mean fluorescence intensity from 10 puncta per retina section was normalized by background. Data are from three images per retina collected from four to six separate mice and represented as mean ± SEM; n = 12 to 18. ****P < 0.0001, one-way ANOVA followed by Tukey's multiple comparisons.

(E) Analysis of synaptic morphology by electron microscopy. Photoreceptor axonal terminals are colored in yellow, processes of horizontal cells in blue, and ON-BC dendrites in pink.

(F) Quantification of synaptic organization features. Rod terminals containing ON-BC dendrites were designated as triads and devoid of ON-BC processes: diads. 188-366 rod terminals from two separate mice were analyzed for each condition. UN, undetermined.

(G) Representative ERG traces elicited by a scotopic flash of 0.001 cd*s/m^2 (~0.6 R*/rod) to activate the primary rod pathway only in *Elfn1*$^{CR/CR}$ mice with subretinal injection of AAV-Cre or control virus.

(H) Quantification of b-wave ERG amplitudes under scotopic conditions. Data are represented as mean ± SEM. n=4-13, ***P < 0.001, one-way ANOVA followed by Tukey's multiple comparisons.

See also Figures S2 and S3.

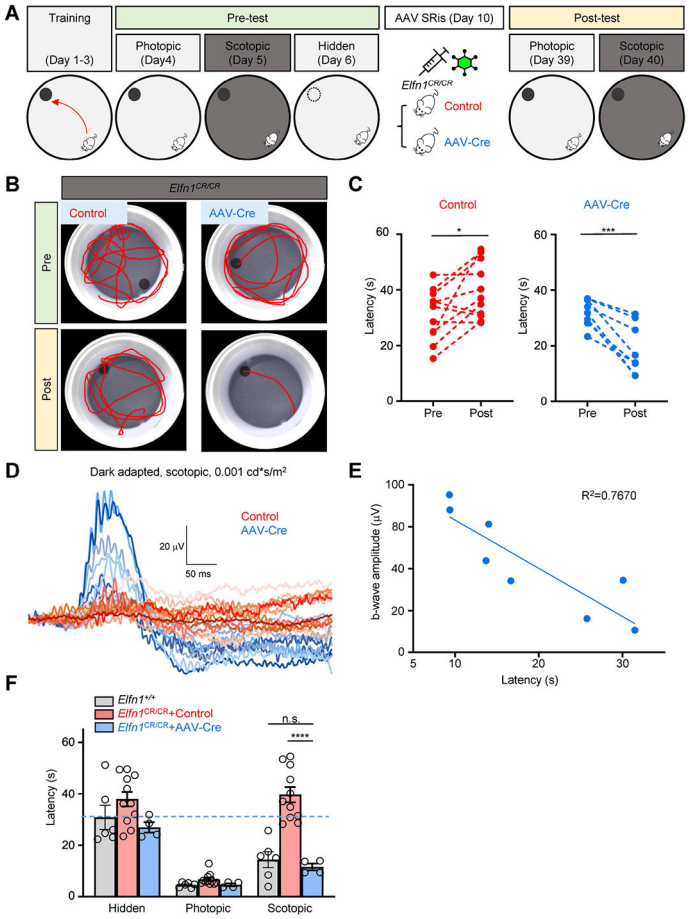

Figure 3. The restoration of Elfn1 in *Elfn1*$^{CR/CR}$ mice enables scotopic vision.

(A) Schematic of the timeline of AAV subretinal treatment and evaluating mouse visual sensitivity to light by a water maze task. Photopic condition (bright gray): 100 cd*s/m^2, Scotopic condition (dark gray): 0.001 cd*s/m^2; SRis, subretinal injections.

(B) Swimming tracks of representative animals during sessions at the scotopic condition (0.001 cd*s/m^2) before and after AAV subretinal injections.

(C) Summary of platform finding latencies at the scotopic condition (0.001 cd*s/m^2) before and after AAV subretinal injections. Data are represented as mean±SEM, n=8-11, *p<0.05, ***p < 0.001, paired t-test.

(D) ERG traces elicited by a scotopic flash of 0.001 cd*s/m^2 (~0.6 R*/rod) to activate the primary rod pathway only in *Elfn1*$^{CR/CR}$ mice with subretinal injection of AAV-Cre (blue) or control virus (red).

(E) Correlation of finding platform latency and b-wave ERG amplitudes in AAV-Cre treated *Elfn1*$^{CR/CR}$ mice. Quantification of data presented in Figs. 3C and 3D.

(F) Summary of platform finding latencies after AAV subretinal injections. Statistical analysis was performed using two-way ANOVA test followed by Turkey's multiple comparisons test. Data are represented as mean± SEM, n=4 to 11, ****p < 0.0001.

See also Figure S4.

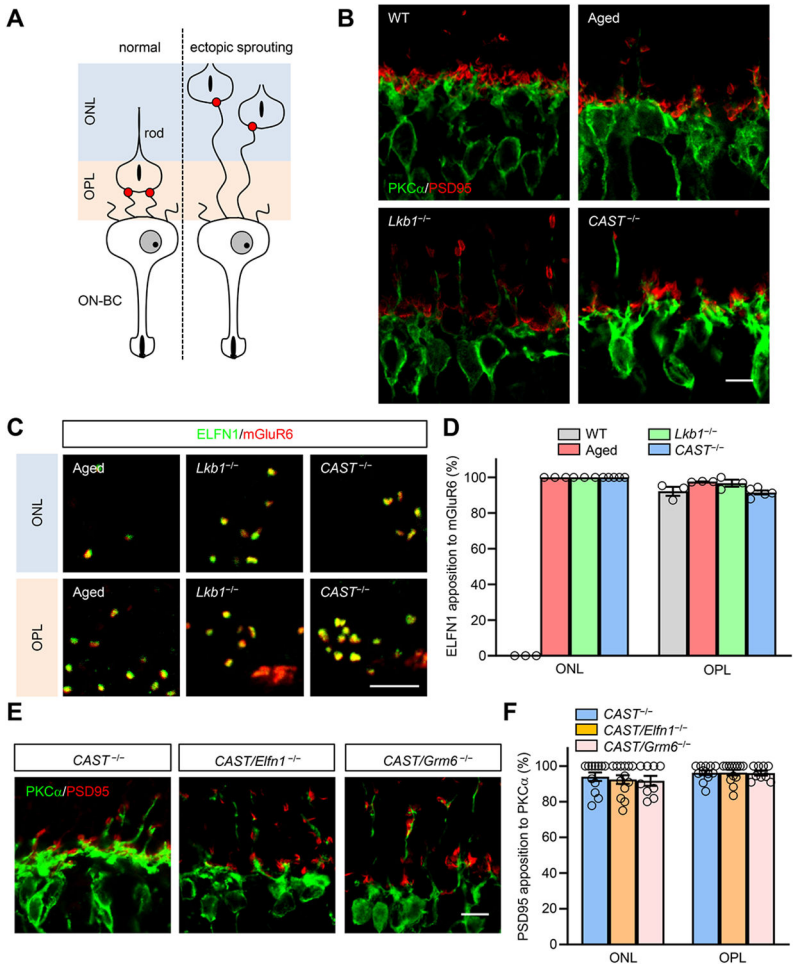

Figure 4. Lamina displacement of axono-dendritic matching preserves trans-synaptic Elfn1-mGluR6 alignment.

(A) Schematic of the rod to ON-BC processes in the normal and ectopically spouting retina. ON-BC to photoreceptor synapses form in the wild-type retinas strictly in the outer plexiform layer (OPL). However, under the conditions that induce axonal retraction, ON-BC dendrites extend all the way to the outer nuclear layer (ONL) to locate the synaptic partner.

(B) Rod bipolar ectopic processes in old wild-type, LKB1-deficient and CAST knockout retinas. Retina cross-sections were double-stained with antibodies against rod ON-BC marker PKCα (green) and pre synaptic marker PSD95 (red). (Scale bar, 5 μm.)

(C) Elfn1-mGluR6 trans-synaptic complex persists at ectopic sites. High magnification of OPL and ONL synapse stained with Elfn1 (green) and mGluR6 (red). (Scale bar, 2.5 μm.)

(D) Statistical analysis of Elfn1 puncta apposed to mGluR6 puncta in OPL and ONL synapse. Data are presented as mean ± SEM. n=3-5.

(E) Elimination of Elfn1 or mGluR6 has no effect on dendritic sprouting in the CAST KO retinas. Retina cross-sections were double immuno-stained with antibodies against PSD95 (red) and PKCα (green). (Scale bar, 2.5 μm.)

(F) Statistical analysis of RBC dendritic tips apposed to the presynaptic terminal in OPL and ONL synapse. Data are presented as mean ± SEM. n=9-13.

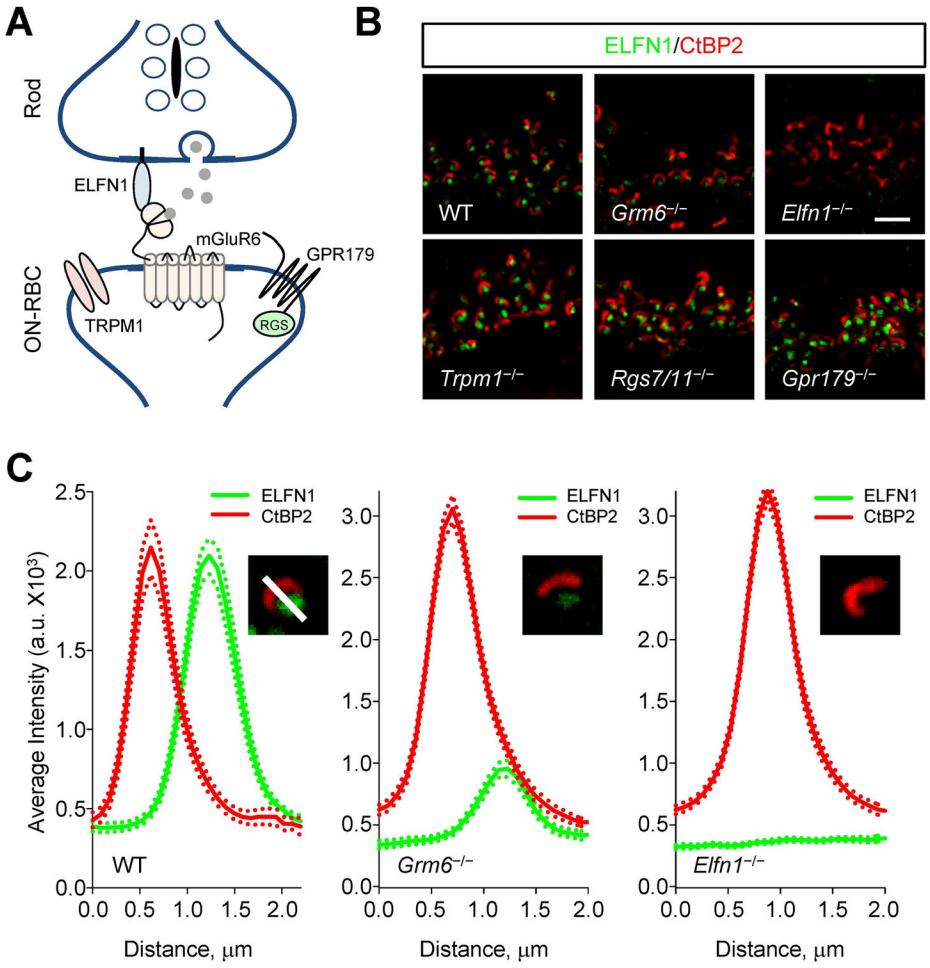

Figure 5. The presynaptic targeting of Elfn1 is independent of the postsynaptic machinery.

(A) Schematic of molecule organization of the first visual synapse.

(B) Effect of eliminating key postsynaptic molecules on expression and localization of Elfn1. Retina cross-sections were double-stained with antibodies against Elfn1 (green) and presynaptic marker CtBP2 (red). Scale bar, 2.5 μm.

(C) Analysis of Efln1 localization in postsynaptic receptor mGluR6 knockout retina. Plots show quantification of relative fluorescence intensity distributions from 10 synaptic puncta. Dashed lines are plots of respective SEM values.

See also Figure S5.

Key resources table

REAGENT or RESOURCE	SOURCE	IDENTIFIER
Antibodies		
Rabbit anti-RGS11	Martemyanov Lab [106]	N/A
Rabbit anti-LRIT3	Dr. Christina Zeits [107]	N/A
Sheep anti-TRPM1	Martemyanov Lab [96]	N/A
Sheep anti-mGluR6	Martemyanov Lab [96]	N/A
Rabbit anti-ELFN1 (NTR)	Martemyanov Lab [68]	N/A
Rabbit anti-$Ca_V1.4$	Dr. Amy Lee [73]	N/A
Mouse anti-CtBP2	BD Biosciences	Cat#612044; RRID:AB_399431
Rabbit anti-PSD95	Cell Signaling Technology	Cat# 3450S; RRID:AB_2292883
Mouse anti-PKCα	Abcam	Cat#ab11723; RRID:AB_298510
Bacterial and virus strains		
AAV8-hGRK1-Cre-P2A-GFP	This paper	N/A
AAV8-hGRK1-GFP	This paper	N/A
Critical commercial assays		
Antigen Retrieval Sampler	R&D System	Cat#CTS016
Experimental Models: Organisms/Strains		
Mouse: *Lrit3*$^{-/-}$	Reference [101]	N/A
Mouse: *GPR179*$^{-/-}$	Reference [102]	N/A
Mouse: *Rgs7/11*$^{-/-}$	Reference [97]	N/A
Mouse: *Elfn1*$^{-/-}$	Reference [68]	N/A
Mouse: *Trpm1*$^{-/-}$	Reference [103]	N/A
Mouse: *Grm6*$^{-/-}$	Riken Bioresource Center	Cat# RBRC05552, RRID:IMSR_RBRC05552
Mouse: *Elfn1*$^{flx/flx}$	Reference [100]	N/A
Mouse: *Elfn1*$^{CR/CR}$	This paper	N/A
Mouse: *Elfn1*^{CreERT2}	This paper	N/A
Mouse: *Elfn1*$^{flx/CreERT2}$	This paper	N/A
Mouse: *Elfn1*$^{CR/CR}$*Pcdh21*^{Cre}	This paper	N/A
Mouse: *LKB1*$^{-/-}$	Reference [70]	N/A
Mouse: *CAST*$^{-/-}$	Reference [98]	N/A
Mouse: *CAST*$^{-/-}$*Elfn1*$^{-/-}$	This paper	N/A
Mouse: *CAST*$^{-/-}$*Grm6*$^{-/-}$	This paper	N/A
Mouse: *Ai14*	The Jackson Laboratory	RRID:IMSR_JAX:007908
Software and algorithms		
EM LKC Technologies software	LKC Technologies	http://www.lkc.com/products/compliance-pack/
Zen2.1 SP1 (Black)	Carl Zeiss	RRID:SCR_013672
MetaMorph image analysis software	Molecular Devices	RRID:SCR_002368

REAGENT or RESOURCE	SOURCE	IDENTIFIER
EthoVision XT	Noldus	RRID:SCR_000441
GraphPad Prism9	GraphPad Software, Inc	RRID:SCR_002798